SUPPLEMENTAL MATERIAL

Identification of a Unique TGF-β Dependent Molecular and Functional Signature in Microglia

Oleg Butovsky[1*], Mark P. Jedrychowski[2], Craig S. Moore[3], Ron Cialic[1], Amanda J. Lanser[1], Galina Gabriely[1], Thomas Koeglsperger[1], Ben Dake[1], Pauline M. Wu[1], Camille E. Doykan[1], Zain Fanek[1], LiPing Liu[5], Zhuoxun Chen[4], Jeffrey D. Rothstein[4], Richard M. Ransohoff[5], Steven P. Gygi[2], Jack P. Antel[3] and Howard L. Weiner[1*]

[1]Center for Neurologic Diseases, Department of Neurology, Brigham and Women's Hospital, Harvard Medical School, Boston, MA 02112.
[2]Department of Cell Biology, Harvard Medical School, Boston, MA 02115, USA.
[3]Neuroimmunology Unit, Montréal Neurological Institute, McGill University, Montréal, Québec, Canada.
[4]Brain Science Institute and Department of Neurology, Johns Hopkins University, Baltimore, Maryland, USA.
[5]Department of Immunology, Cleveland Clinic, Cleveland, Ohio, USA.

Nature Neuroscience: doi:10.1038/nn.3599

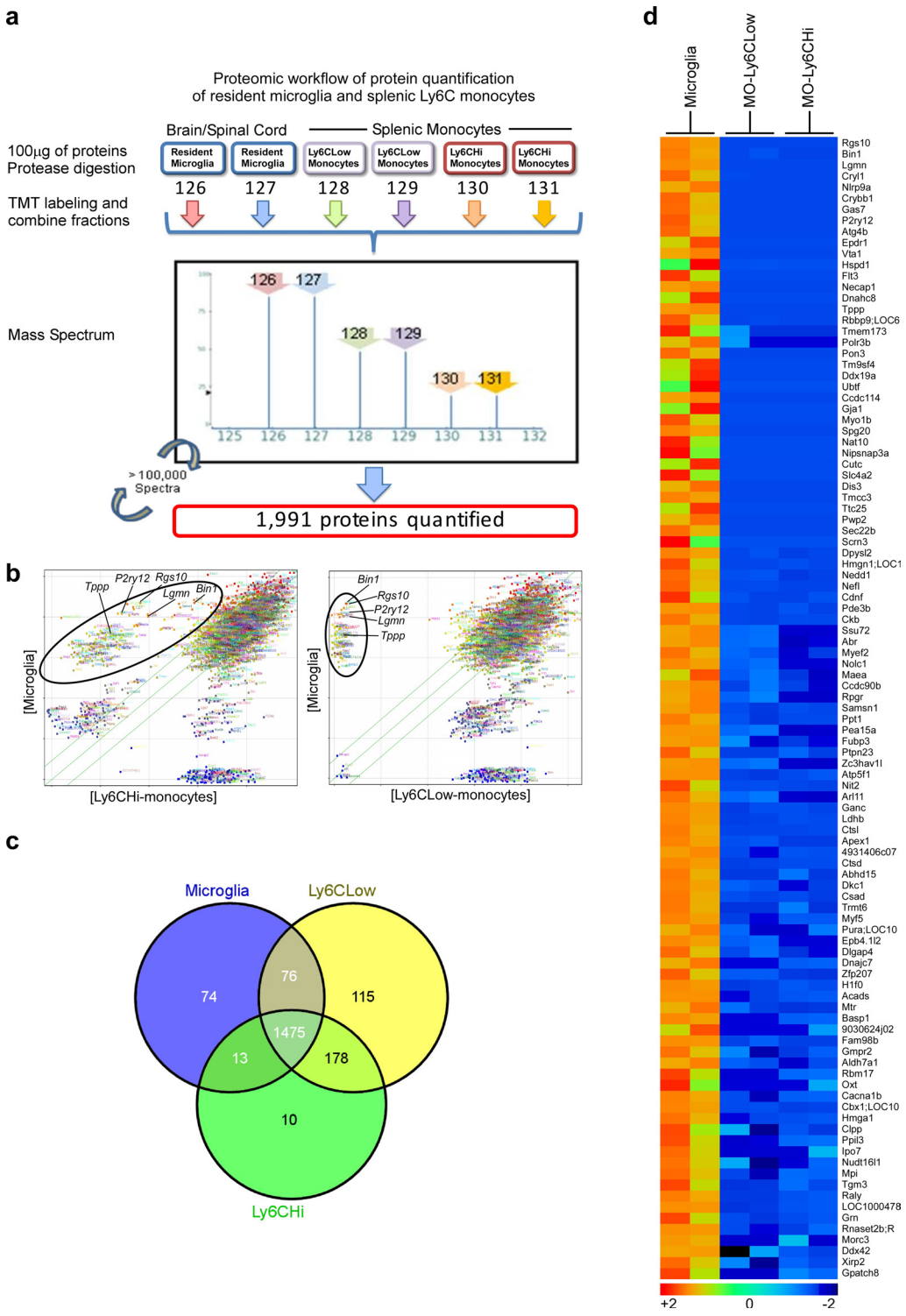

Supplementary Figure 1. Identification of protein signature in microglia and Ly6C monocyte subsets. (a) Schematic representation of the workflow for TMT-based quantitative proteomic analysis of microglia and splenic Ly6C monocytes. **(b)** Protein expression scatter plot of microglia versus monocytes subsets. **(c)** Venn diagram of unique and common proteins in microglia vs. Ly6C^{Hi} and Ly6C^{Low} monocytes. **(d)** Heatmap of 103 enriched microglia proteins (>5-fold).

Nature Neuroscience: doi:10.1038/nn.3599

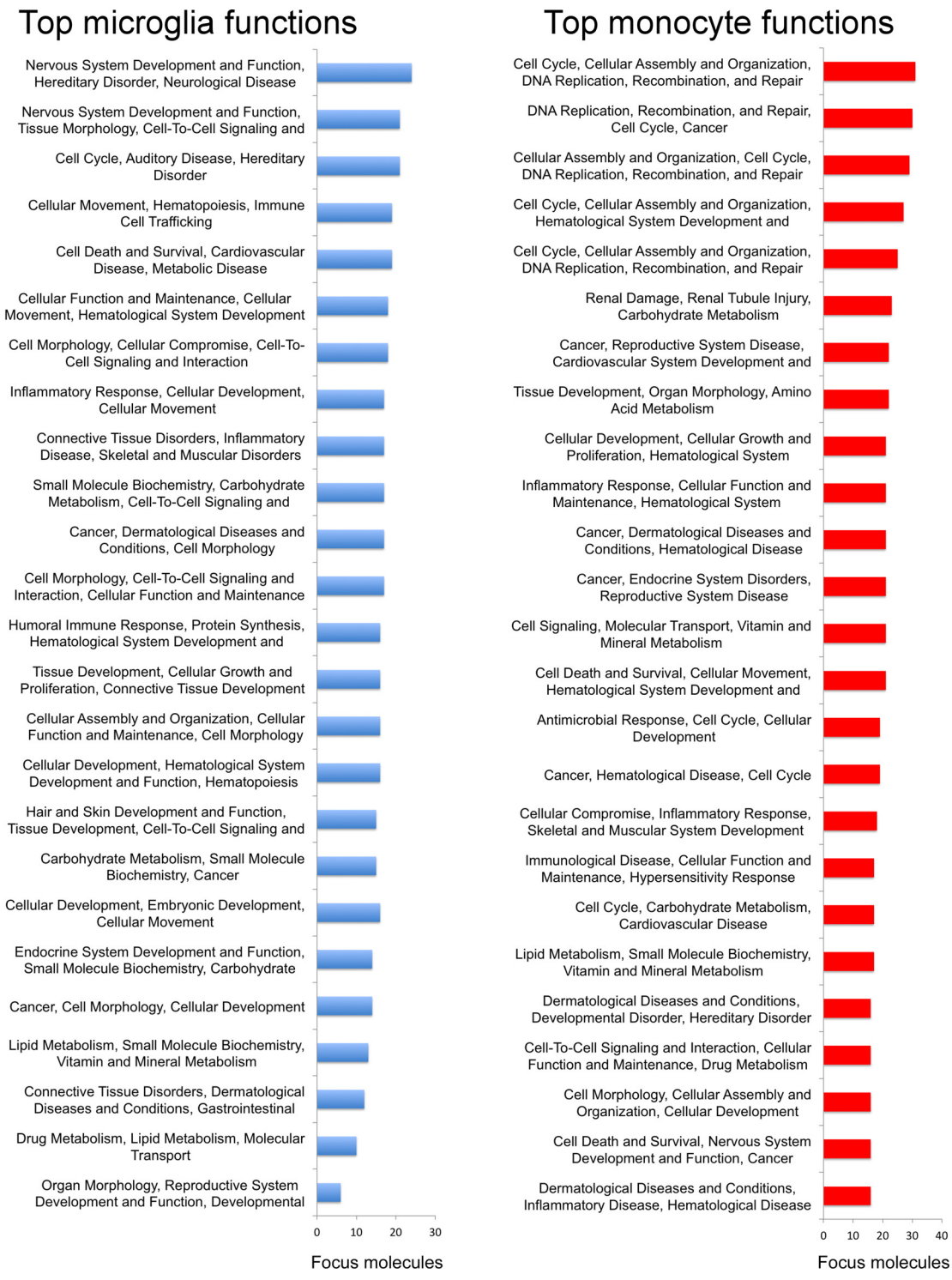

Supplementary Figure 2. Top biological functions in microglia. Microglia and monocyte gene signature identified by AffyExon1 arrays (see Fig. 1a) were analyzed by Ingenuity pathway analysis (IPA™). Bars indicate molecules present in dataset for each function.

Nature Neuroscience: doi:10.1038/nn.3599

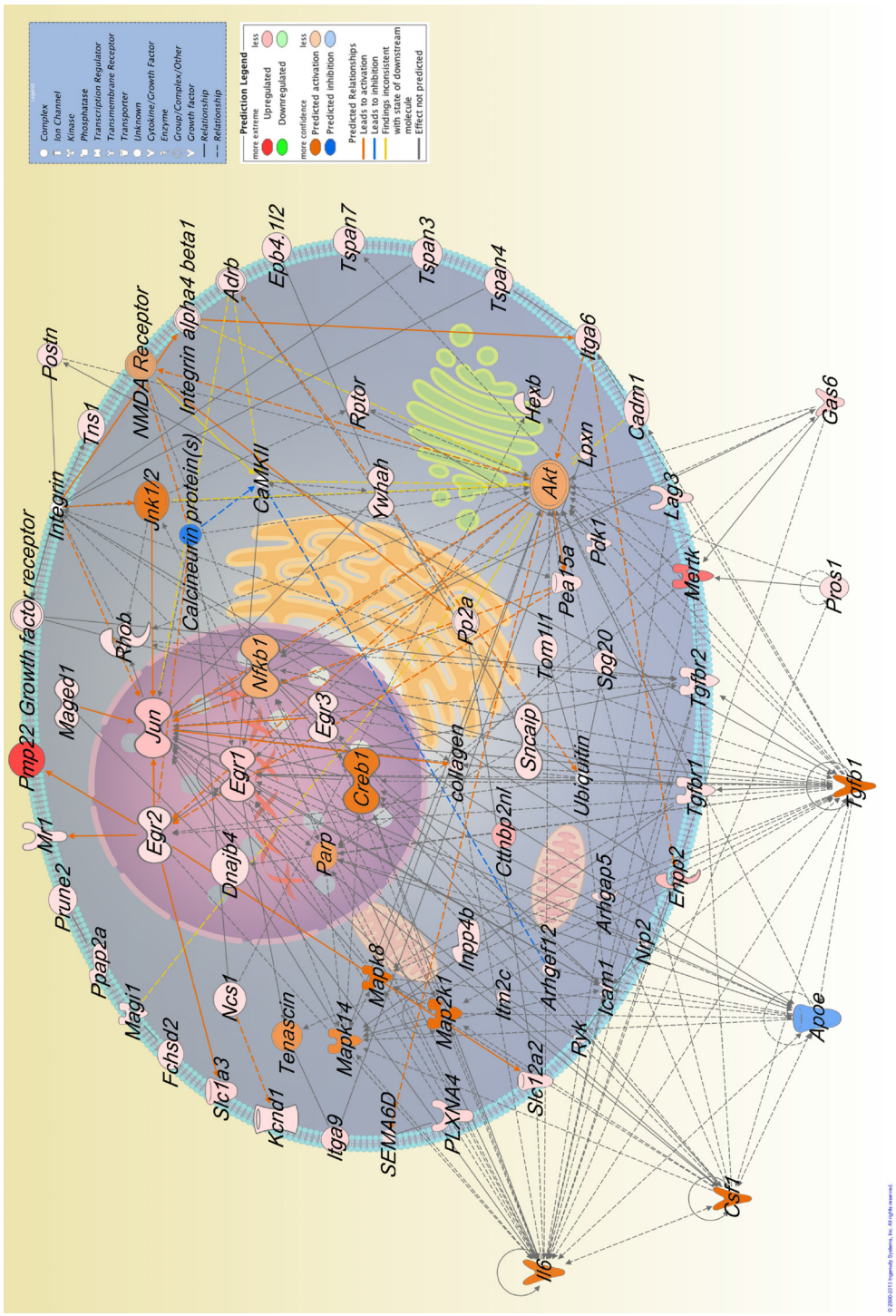

Supplementary Figure 3. Nervous system development and function in microglia. The subcellular localization of top microglial functions genes from Supplementary Figure 2 (Nervous system development and function, hereditary disorders, neurological disease genes) are illustrated. For each molecule in the dataset the expression fold change as compared to monocytes, P value and normalized expression level are presented.

Nature Neuroscience: doi:10.1038/nn.3599

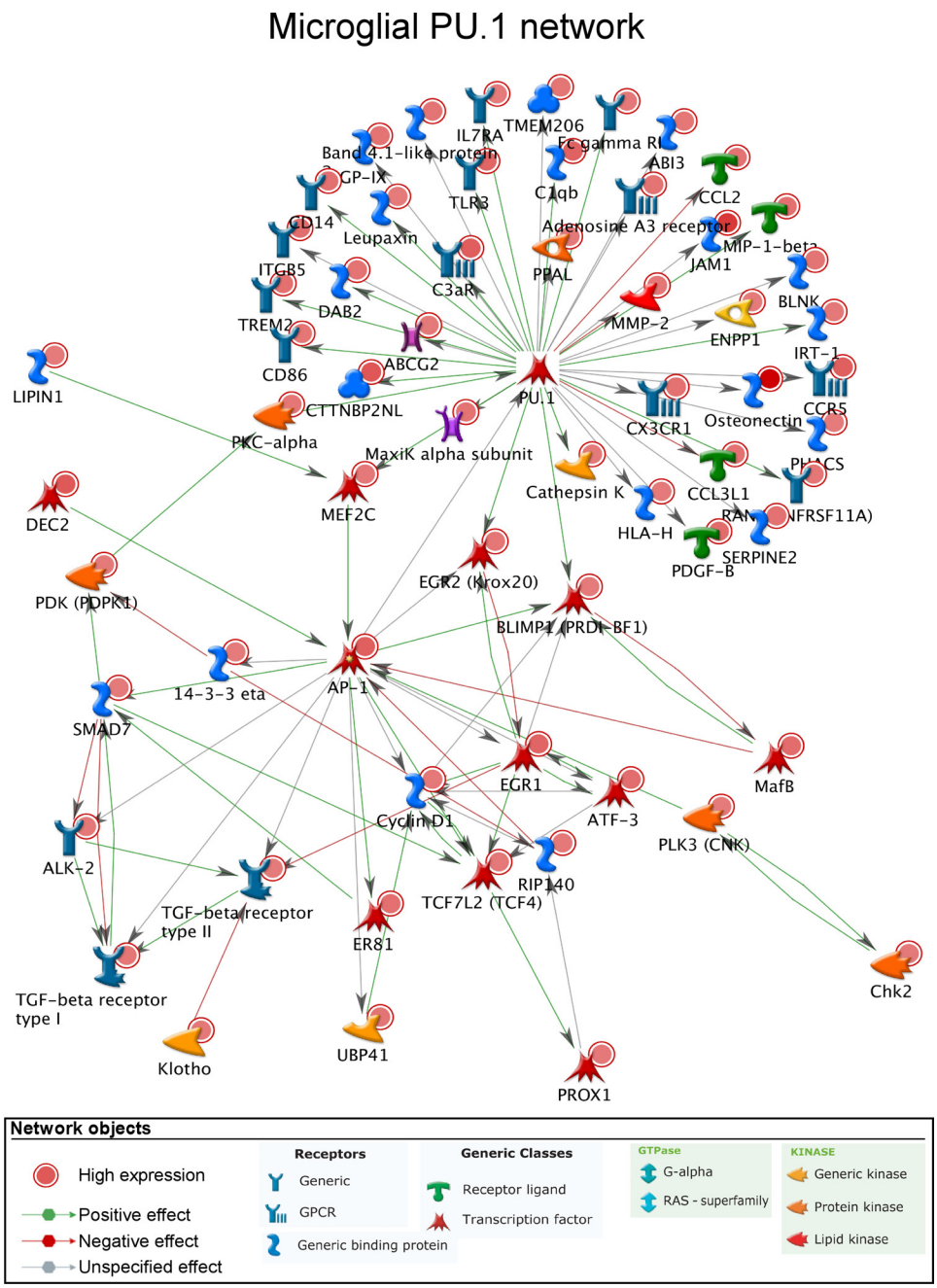

Supplementary Figure 4. Top microglial interactions by protein function. Illustration of microglial PU.1 network.

Nature Neuroscience: doi:10.1038/nn.3599

Supplementary Figure 5. Canonical pathways in microglia and monocytes. Microglial and monocytes gene signatures identified with AffyExon1 arrays were analyzed by IPA™ for canonical pathways. Bars indicate –log P value (ratio of molecules present in the dataset out of all the function related molecules).

Nature Neuroscience: doi:10.1038/nn.3599

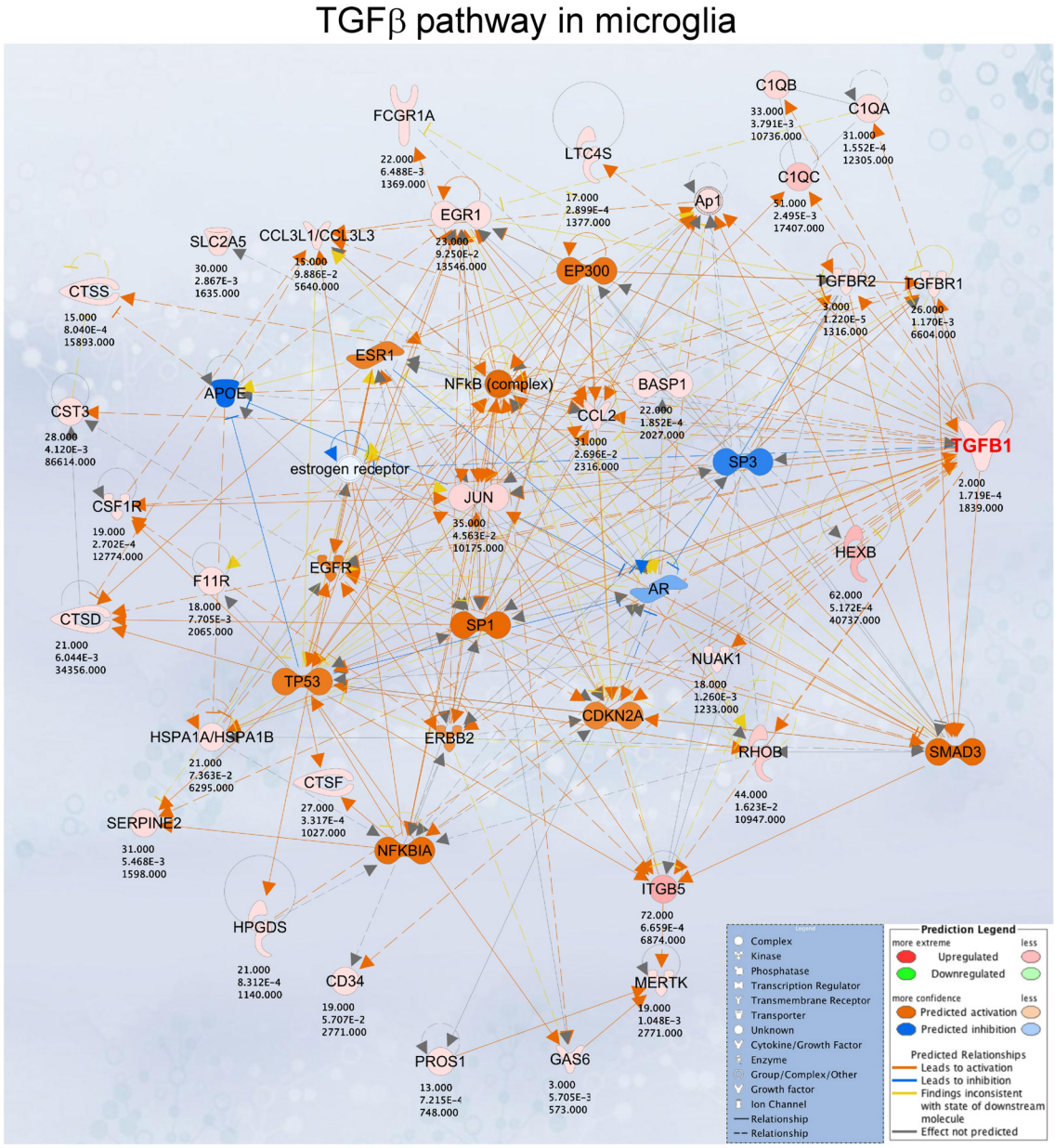

Supplementary Figure 6. TGF-β pathway in microglia. For each molecule in the dataset the expression fold change as compared to monocytes, P value and normalized expression level are presented.

Nature Neuroscience: doi:10.1038/nn.3599

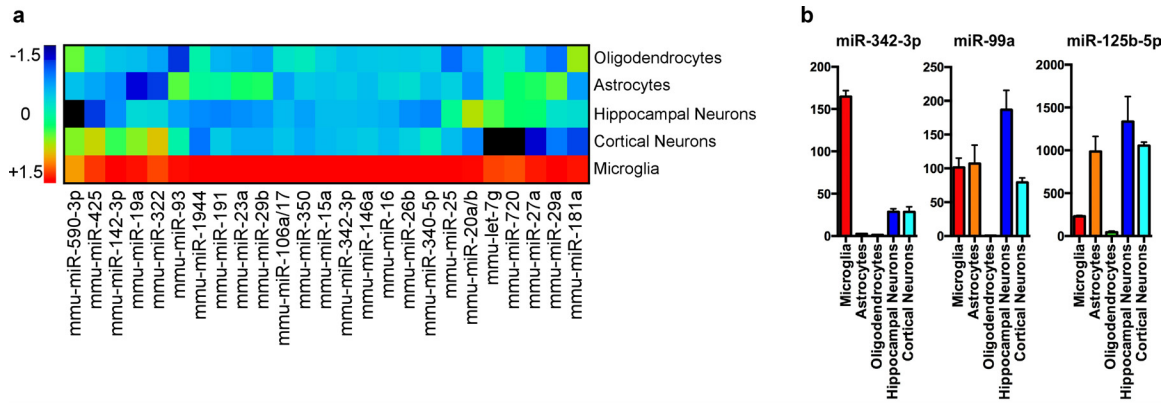

Supplementary Figure 7. miRNA profile in microglia vs. astrocytes, oligodendrocytes and neurons. (a) Heatmap of biological duplicates for FCRLS^{+} adult microglia (n = 5 mice), Glt-EGFP^{+} adult astrocytes (n = 9 mice), adult oligodendrocytes (n = 5 mice) and primary postnatal hippocampal and cortical neurons. Top 25 enriched miRNAs in microglia are presented (full miRNA list, Source data – Supplementary Figure 7). Each lane represents the average expression value of two biological duplicates per cell type. **(b)** qPCR analysis of microglia enriched miRNAs (miR-342-3p, miR-99a and miR-125b-5p) in CNS cell type. miRNA expression level was normalized against U6 miRNA using ΔCt. Bars show mean ±SEM. Shown is one of two individual experiments.

Nature Neuroscience: doi:10.1038/nn.3599

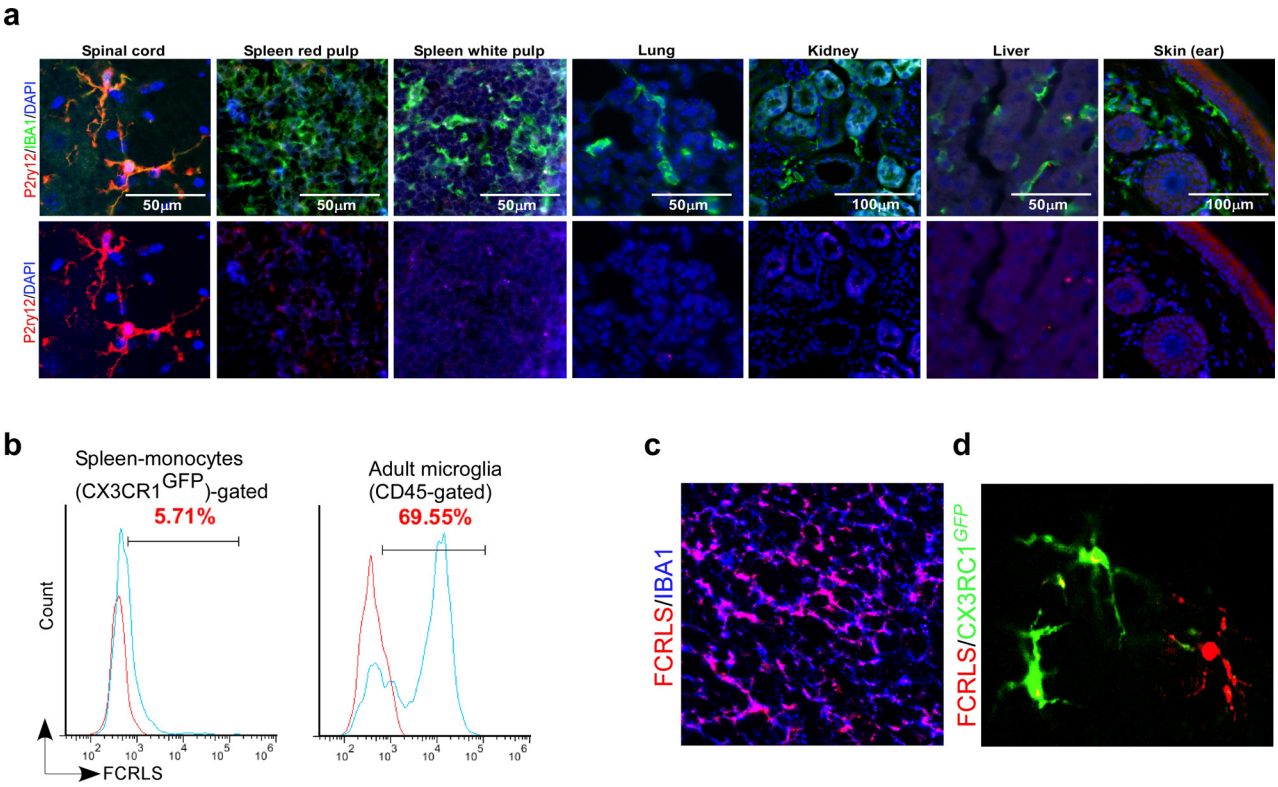

Supplementary Figure 8. Specificity of P2ry12 and FCRLS antibodies in resident microglia. (a) Immonohistochemical analysis of mouse spinal cord, spleen red and pulp, lung, kidney, liver and skin (ear) stained with anti-P2ry12 (microglia; red), anti-Iba-1 (myeloid cells; green) and DAPI (nucleus; blue). Representative images of 5 mice. **(b)** FACS analysis of FCRLS surface expression in splenic CX3CR1$^{GFP/+}$ monocytes and CD11b/CD45^{+} brain microglia. **(c** and **d)** Confocal images of mouse brain stained with Iba-1 and polyclonal FCRLS antibody in **(c)** naïve and **(d)** chimeric CX3CR1$^{GFP/+}$ mice. Anti-FCRLS signal co-localized with Iba-1^{+} microglia and does not stain recruited monocytes in the brain of CX3CR1^{GFP} chimeric mouse transplanted with bone marrow derived cells from CX3CR1$^{GFP/+}$ transgenic mice.

Nature Neuroscience: doi:10.1038/nn.3599

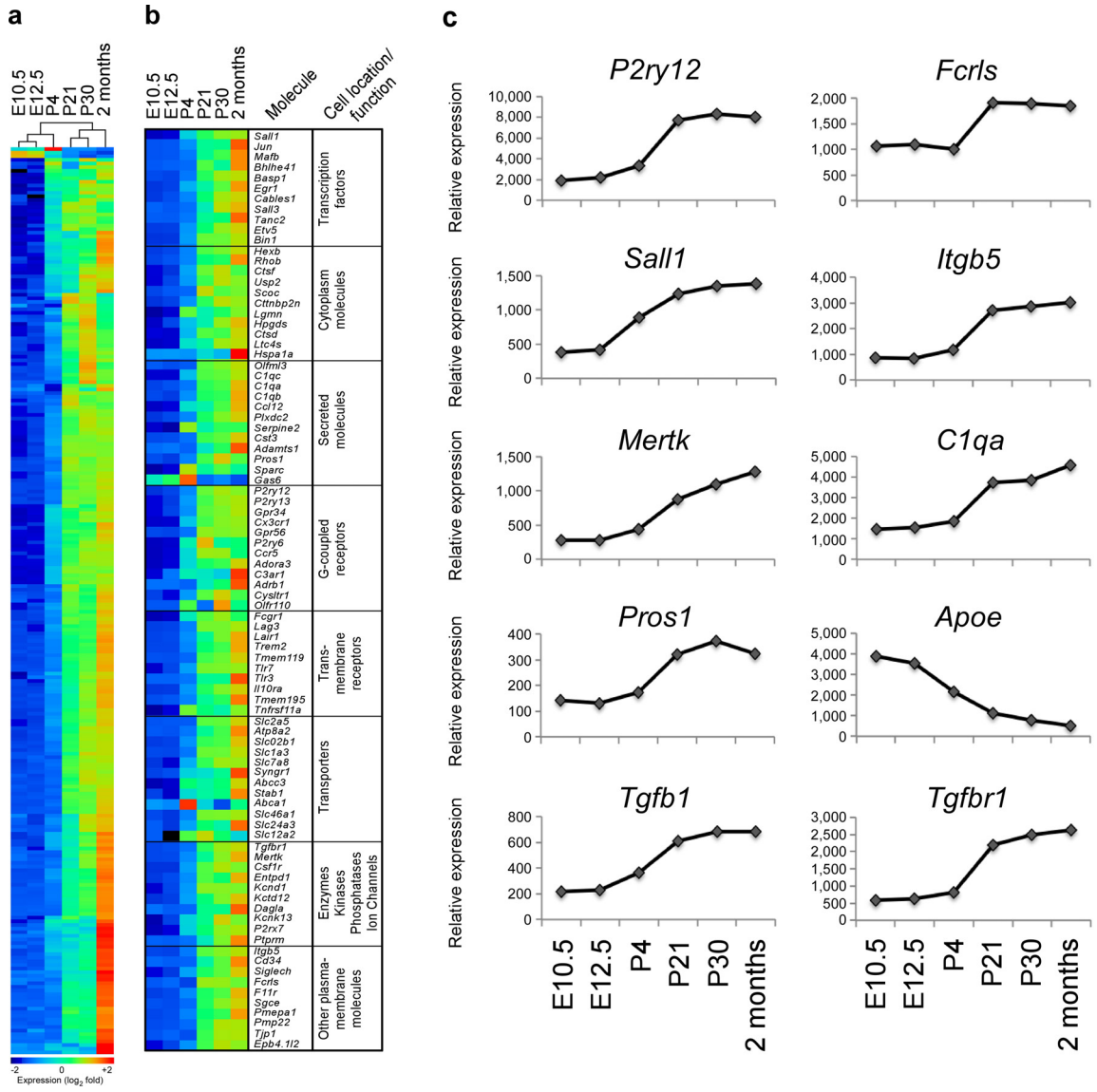

Supplementary Figure 9. Microglia signature during development. **(a)** MG400 expression profile of microglia from mice bran at E10.5, E12.5, P3, P21, P30 and 2 months of age (full gene list, Source data – Supplementary Figure 9). Results were log-transformed, normalized (to the mean expression of zero across samples) and centered, and populations and genes were clustered by pairwise centroid linkage with the Pearson correlation. Data are pooled of 2 different experiments; E10.5 (n = 10), E12.5 (n = 10), P4 (n = 8), P21 (n = 5), P30 (n = 5) and 2 months (n = 5). **(b)** Top microglial molecules grouped according to cell localization and function. **(c)** qPCR analysis of 6 selected microglia genes in MCSF+TGF-β1 cultured microglia. Gene expression level was normalized against *Gapdh* using ΔCt.

Nature Neuroscience: doi:10.1038/nn.3599

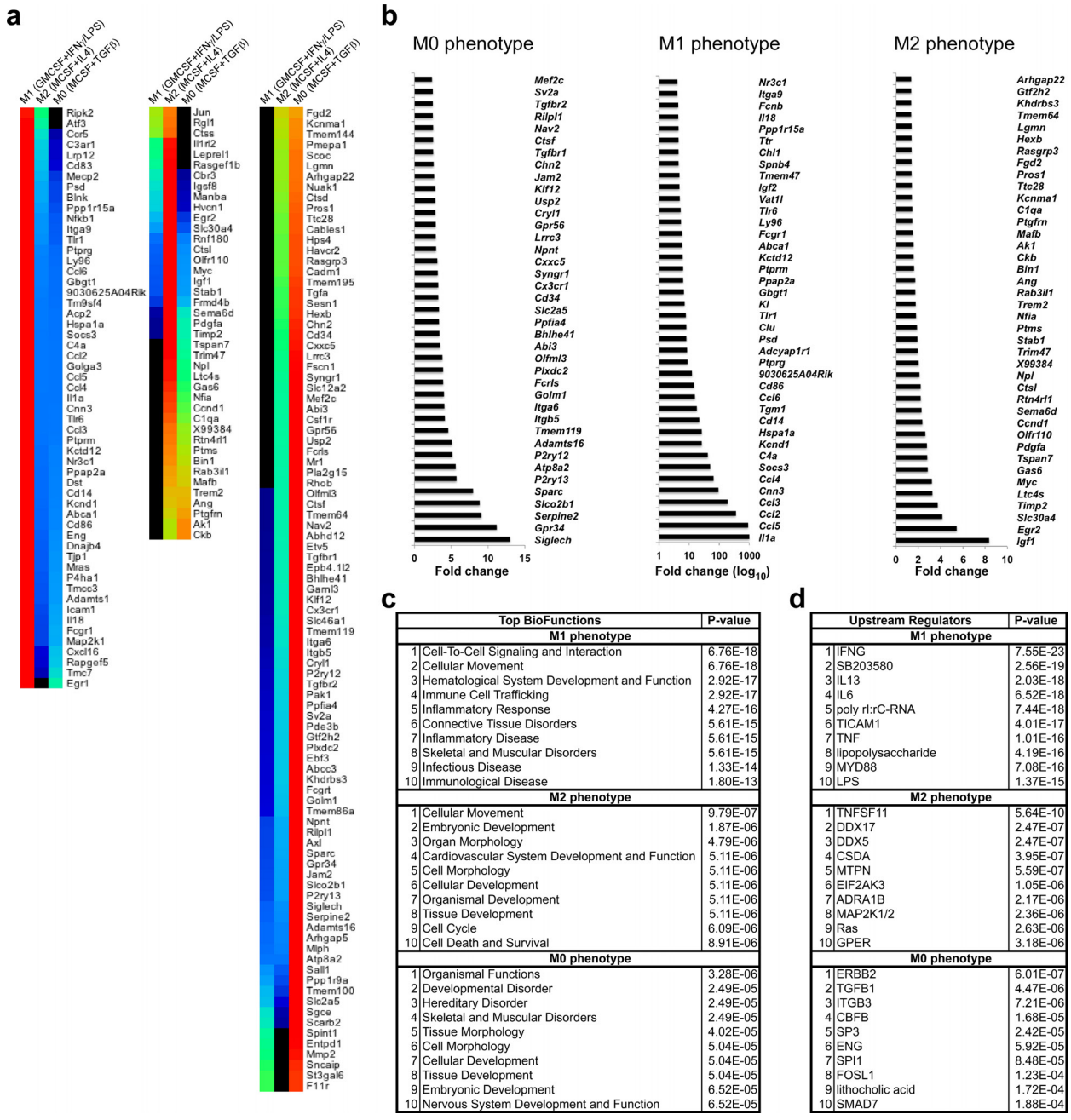

c

Top BioFunctions	P-value
M1 phenotype	
1 Cell-To-Cell Signaling and Interaction	6.76E-18
2 Cellular Movement	6.76E-18
3 Hematological System Development and Function	2.92E-17
4 Immune Cell Trafficking	2.92E-17
5 Inflammatory Response	4.27E-16
6 Connective Tissue Disorders	5.61E-15
7 Inflammatory Disease	5.61E-15
8 Skeletal and Muscular Disorders	5.61E-15
9 Infectious Disease	1.33E-14
10 Immunological Disease	1.80E-13
M2 phenotype	
1 Cellular Movement	9.79E-07
2 Embryonic Development	1.87E-06
3 Organ Morphology	4.79E-06
4 Cardiovascular System Development and Function	5.11E-06
5 Cell Morphology	5.11E-06
6 Cellular Development	5.11E-06
7 Organismal Development	5.11E-06
8 Tissue Development	5.11E-06
9 Cell Cycle	6.09E-06
10 Cell Death and Survival	8.91E-06
M0 phenotype	
1 Organismal Functions	3.28E-06
2 Developmental Disorder	2.49E-05
3 Hereditary Disorder	2.49E-05
4 Skeletal and Muscular Disorders	2.49E-05
5 Tissue Morphology	4.02E-05
6 Cell Morphology	5.04E-05
7 Cellular Development	5.04E-05
8 Tissue Development	5.04E-05
9 Embryonic Development	6.52E-05
10 Nervous System Development and Function	6.52E-05

d

Upstream Regulators	P-value
M1 phenotype	
1 IFNG	7.55E-23
2 SB203580	2.56E-19
3 IL13	2.03E-18
4 IL6	6.52E-18
5 poly rI:rC-RNA	7.44E-18
6 TICAM1	4.01E-17
7 TNF	1.01E-16
8 lipopolysaccharide	4.19E-16
9 MYD88	7.08E-16
10 LPS	1.37E-15
M2 phenotype	
1 TNFSF11	5.64E-10
2 DDX17	2.47E-07
3 DDX5	2.47E-07
4 CSDA	3.95E-07
5 MTPN	5.59E-07
6 EIF2AK3	1.05E-06
7 ADRA1B	2.17E-06
8 MAP2K1/2	2.36E-06
9 Ras	2.63E-06
10 GPER	3.18E-06
M0 phenotype	
1 ERBB2	6.01E-07
2 TGFB1	4.47E-06
3 ITGB3	7.21E-06
4 CBFB	1.68E-05
5 SP3	2.42E-05
6 ENG	5.92E-05
7 SPI1	8.48E-05
8 FOSL1	1.23E-04
9 lithocholic acid	1.72E-04
10 SMAD7	1.88E-04

Supplementary Figure 10. M0, M1 and M2 microglial phenotypes as measured by MG400 chip. **(a)** Heatmap of significantly affected MG400 genes in M0, M1 and M2 polarized microglia. One representative of three individual experiments is shown. **(b)** Top 40 affected genes in M0, M1 and M2 microglia. Bars represent fold change as compared to the other two phenotypes. **(c** and **d)** IPA™ analysis of **(c)** top bio functions and **(d)** Top upstream regulators in M0-, M1- and M2-polarized microglia.

Nature Neuroscience: doi:10.1038/nn.3599

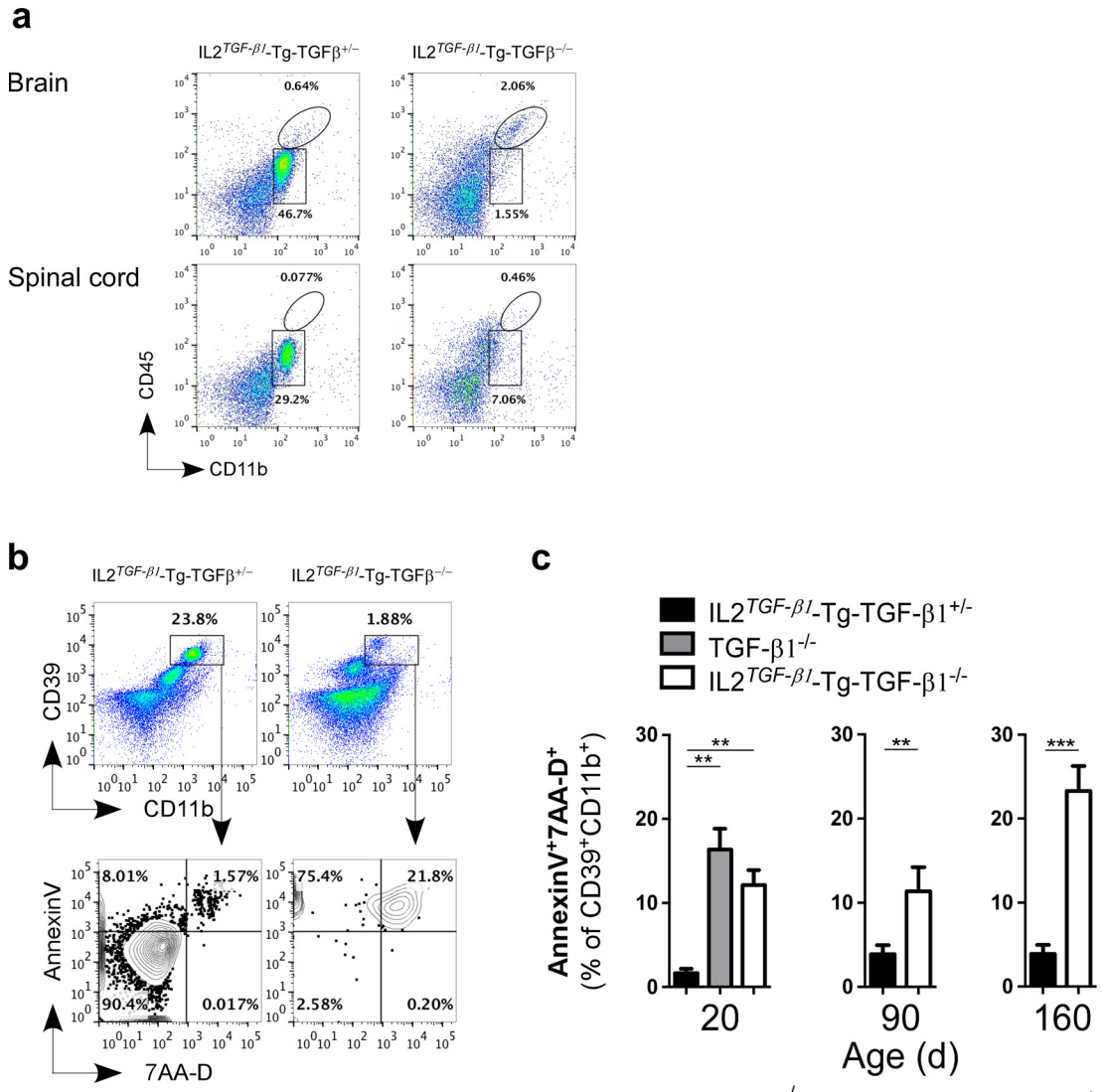

Supplementary Figure 11. Microglia loss in CNS-TGFβ1$^{-/-}$ mice. (a) Representative FACS analysis of isolated brain- and spinal cord-derived mononuclear cells stained with CD45 and CD11b antibodies at 160d of age in IL2^{TGFβ1}-Tg-TGF-β1$^{+/-}$ (n = 6) and IL2^{TGFβ1}-Tg-TGF-β1$^{-/-}$ (n = 6) mice. **(b** and **c)** Increased apoptosis of CD39^{+}CD11b^{+} cells in the brain of CNS-TGF β 1$^{-/-}$ mice. **(b)** Representative FACS analysis of isolated brain-derived mononuclear cells for apoptosis as measured by AnnexinV and 7AA-D in CD39^{+}CD11b^{+}-gated cells at 160d of age in IL2^{TGFβ1}-Tg-TGF-β1$^{+/-}$ (left) and IL2^{TGFβ1}-Tg-TGF-β1$^{-/-}$ (right) mice. **(c)** Quantitative analysis of AnnexinV^{+}7AAD^{+} cell as percentage of CD39^{+}CD11b^{+} cells in TGF-β1$^{-/-}$, IL2$^{TGF-β1}$-Tg-TGF-β1$^{+/-}$ and IL2$^{TGF-β1}$-Tg-TGF-β1$^{-/-}$ mice at 20 (n = 6), 90 (n = 5) and 160 (n = 5) days. Data represent mean ± s.e.m. **P<0.01, $F_{2,6}$=2.146 1-Way ANOVA followed by Dunnett's multiple-comparison *post-hoc* test for comparison at 20d and **P<0.01, t=4.51 and ***P<0.001, t=13.84; Student's t test, 2-tailed for comparison at 90d and 160d.

Nature Neuroscience: doi:10.1038/nn.3599

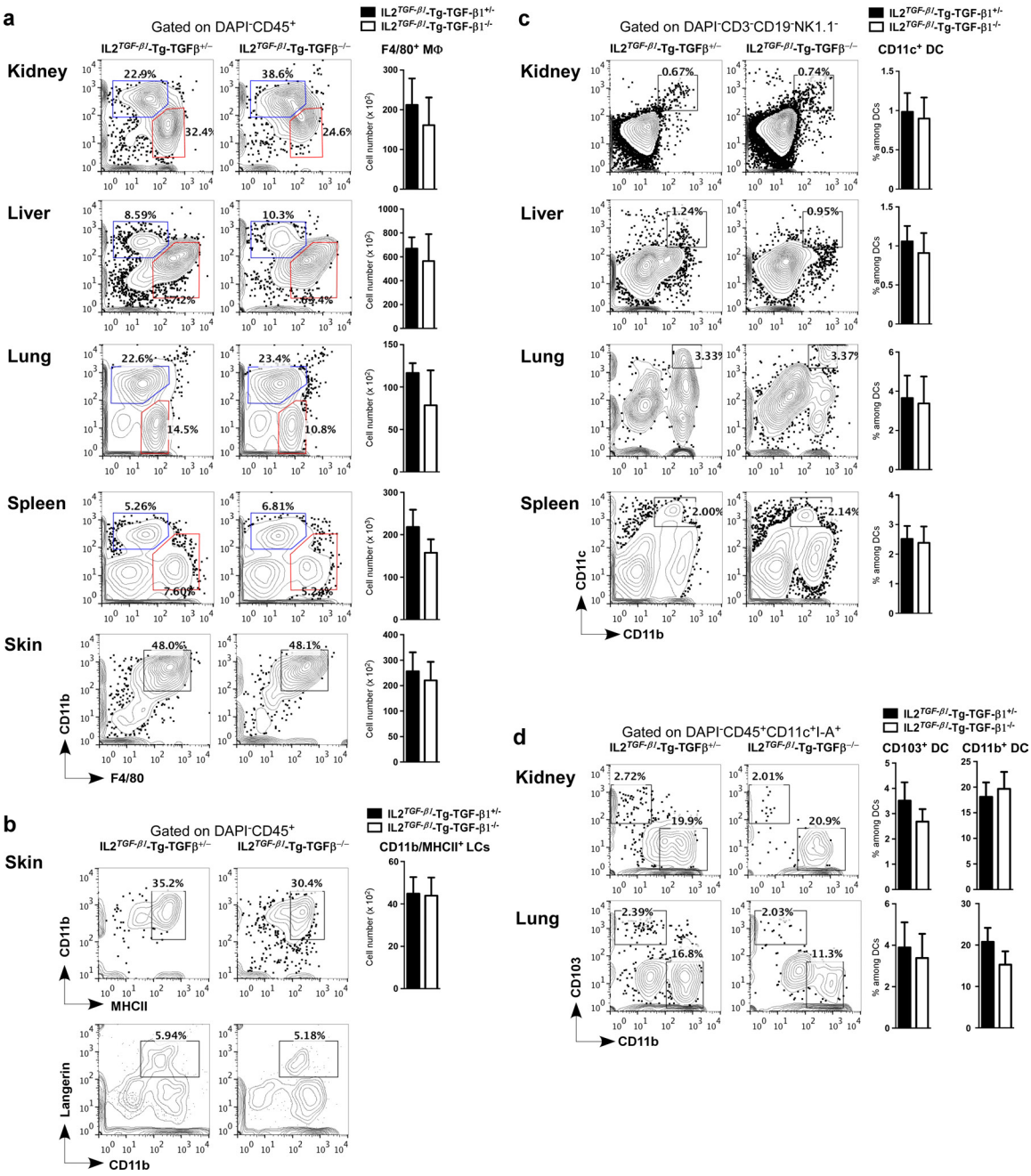

Supplementary Figure 12. Macrophages, dendritic cells and Langerhans cells are not affected in peripheral organs of CNS-TGFβ1$^{-/-}$ mice. (a-d) Nonlymphoid and lymphoid tissue myeloid cells isolated from IL2^{TGFβ1}-Tg-TGF-β1$^{+/-}$ (left) and IL2^{TGFβ1}-Tg-TGF-β1$^{-/-}$ (right) mice at 160d were analyzed by flow cytometry. FACS representative dot plots show the percentage and absolute numbers of **(a)** kidney, liver, lung, spleen and skin derived CD11b^{+}F4/80^{+} macrophages and **(b)** Langerhans cell (LC) stained with MHCII^{+}CD11b^{+} and Langerin^{+}CD11b^{+} in the ear skin cell suspension among DAPI^{-}CD45^{+} cells of IL2^{TGFβ1}-Tg-TGF-β1$^{+/-}$ (n = 6) and IL2^{TGFβ1}-Tg-TGF-β1$^{-/-}$ (n = 6) mice. **(c)** Plots show percentage of CD11c^{+} DCs among gated DAPI^{-}CD3^{-}CD19^{-}NK1.1^{+} cells. **(d)** Dot plots show percentage of CD103^{+} and CD11b^{+} DCs among gated DAPI^{-}CD45^{+}CD11c^{+}I-A^{+} cells. Bars represent data from 2 pooled experiments. Errors bars represent ± s.e.m.

Nature Neuroscience: doi:10.1038/nn.3599

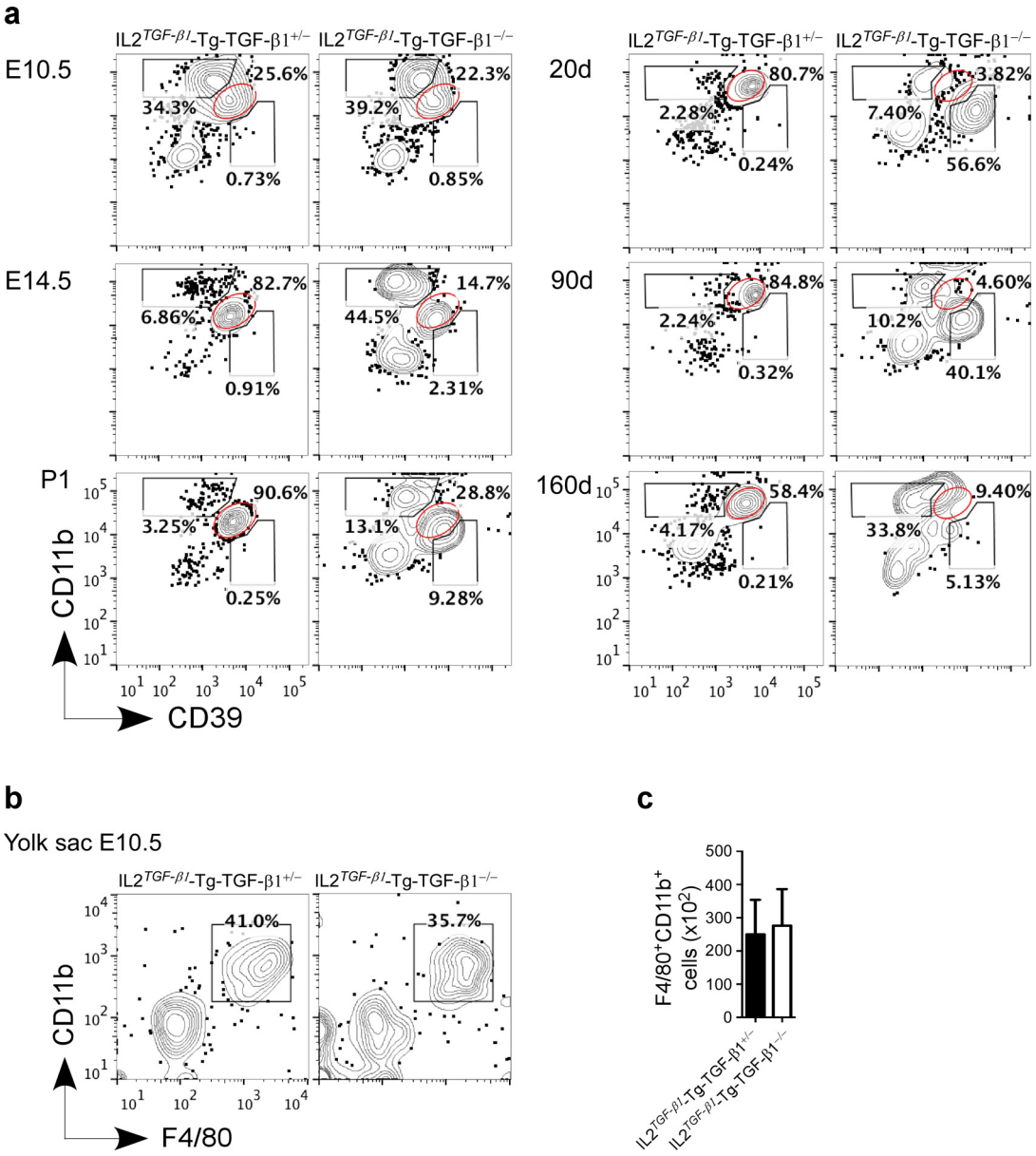

Supplementary Figure 13. Loss of microglia during development in CNS-TGF-β1 deficient mice. (a) FACS analysis of CD39 and CD11b expression among $CD45^+$ cells in the brain during development and aging in $IL2^{TGF\text{-}\beta1}$-Tg-TGF-$\beta1^{+/-}$ and $IL2^{TGF\text{-}\beta1}$-Tg-TGF-$\beta1^{-/-}$ mice at E10.5 (n = 4), E14.5 (n = 5), P1 (n = 5), 20d (n = 6), 90d (n = 5), 160d (n = 5). **(b)** FACS plots show the percentage among $CD45^+$ cells and **(c)** total cell number ± s.e.m. of $F4/80^+CD11b^+$ primitive macrophages in the yolk sac at E10.5 in $IL2^{TGF\text{-}\beta1}$-Tg-TGF-$\beta1^{+/-}$ (n = 6) and $IL2^{TGF\text{-}\beta1}$-Tg-TGF-$\beta1^{-/-}$ (n = 10) mice. P=0.74, t=0.35 Student's t test, 2-tailed.

Nature Neuroscience: doi:10.1038/nn.3599

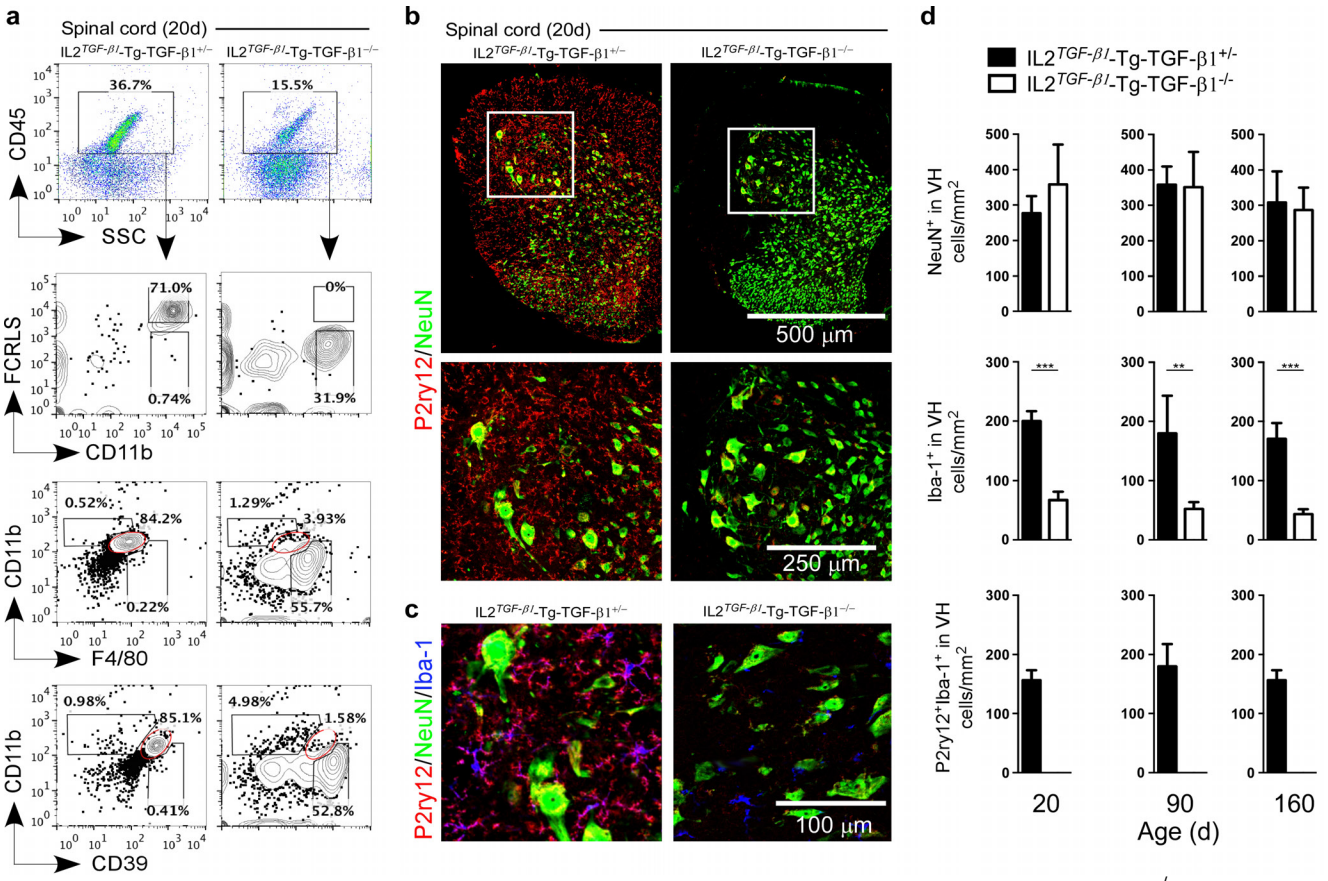

Supplementary Figure 14. Microglia loss in the spinal cord of CNS-TGFβ1$^{-/-}$ mice. (a) Representative FACS analysis of isolated spinal cord-derived mononuclear cells stained for FCRLS, F4/80, CD39 and CD11b among hematopoietic (CD45^{+}) cells at 20d of age in in IL2$^{TGF\text{-}\beta1}$-Tg-TGF-β1$^{+/-}$ and IL2$^{TGF\text{-}\beta1}$-Tg-TGF-β1$^{-/-}$ mice). Immonohistochemical analysis of mouse spinal cord axial section of lumbar level stained with **(b)** anti-P2ry12 (microglia) and anti-NeuN (neurons) and **(c)** anti-P2ry12 (microglia), Iba-1 (myeloid cells) and anti-NeuN (neurons) at 20 days of age (IL2$^{TGF\text{-}\beta1}$-Tg-TGF-β1$^{+/-}$ and IL2$^{TGF\text{-}\beta1}$-Tg-TGF-β1$^{-/-}$) mice. Representative images of 3-5 mice. Scale bar represents 500µm (top panel) and 250µm (zoomed are indicated, bottom panel). **(d)** Quantitative analysis of NeuN^{+}, Iba-1^{+} and P2ry12+/Iba-1^{+} cells in IL2$^{TGF\text{-}\beta1}$-Tg-TGF-β1$^{+/-}$ and IL2$^{TGF\text{-}\beta1}$-Tg-TGF-β1$^{-/-}$ mice at 20, 90 and 160 days of age. Data represent mean ± s.e.m (n = 5). ***P*<0.01, ****P*<0.001, Student's *t* test, 2-tailed.

Nature Neuroscience: doi:10.1038/nn.3599

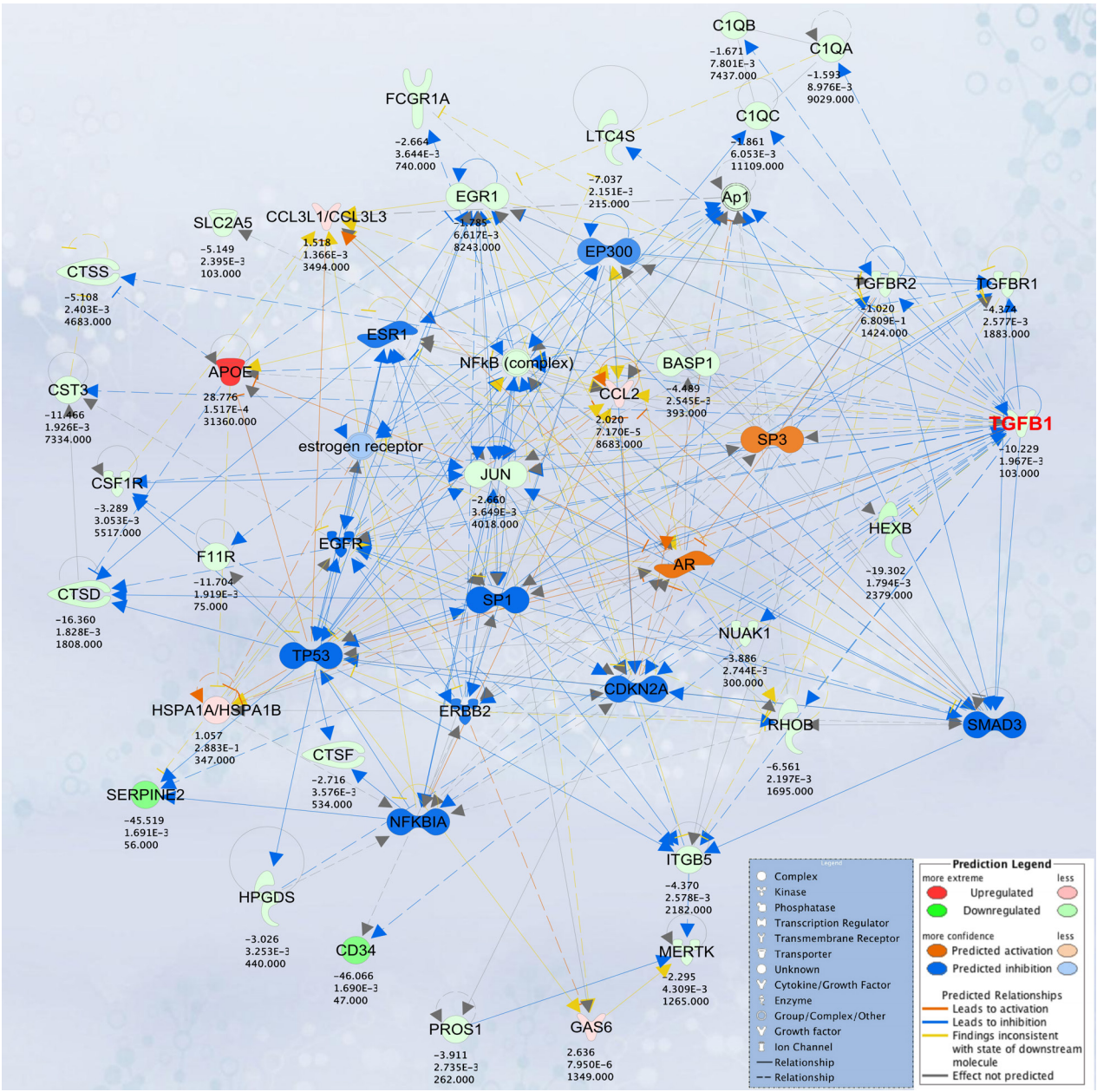

Supplementary Figure 15. TGF-β pathway and downstream microglial molecules are suppressed in CNS-TGFβ1$^{-/-}$ mice. For each molecule in the dataset the expression fold change as compared to microglia from IL2$^{TGF\text{-}\beta 1}$-Tg-TGF-β1$^{+/-}$ mice, P value and normalized expression level are presented.

Nature Neuroscience: doi:10.1038/nn.3599

Supplementary Table 1:
Top 25 enriched genes in each cell type based on hierarchical clustering

	GeneName	Microglia	Astrocytes	Oligodendrocytes	Cort.Neurons	Hipp.Neurons
Oligodendrocytes	*Enpp2*	17	307	13613	34	24
	Ptgds	10	52	4343	14	5
	Aplp1	15	976	11980	775	1130
	Ncam1	4	881	1521	334	354
	Ttr	10	98	1470	17	11
	Omg	7	619	1366	157	76
	Gpm6b	22	4040	4657	1000	1643
	Qdpr	79	136	5210	136	213
	Slc12a2	68	38	1295	36	20
	Kcnk13	81	7	320	27	11
	Tmeff1	11	19	457	126	109
	Chn2	92	9	401	36	40
	App	130	440	5319	564	785
	Dip2a	14	53	411	29	29
	Tppp	82	86	1641	116	194
	Gab1	139	159	1160	46	60
	Kl	16	20	200	23	7
	Slc4a2	42	47	384	26	15
	Sv2a	27	88	1025	251	252
	Tmcc3	83	63	450	25	26
	Frmd4b	199	30	222	13	11
	Gas7	9	146	350	240	201
	Bin1	407	35	715	69	71
	Sema6d	11	167	190	18	14
	Tmem144	75	60	209	20	9
Astrocytes	*Ptprz1*	2	2144	104	397	546
	Clu	8	7418	842	419	639
	Gpr37l1	12	3047	131	26	5
	Gpm6a	10	3263	130	1305	1654
	Slc6a1	6	1373	193	156	96
	Tmem47	6	861	93	147	156
	Slc1a3	257	16656	425	670	1266
	Abcb4	5	643	295	276	323
	Nrcam	6	319	19	146	268
	Apoe	368	11630	2882	851	1672
	Il18	55	404	79	18	21
	Tspan7	65	1428	120	184	280
	Chi3l1	8	102	16	15	6
	Axl	11	131	13	17	14
	Cables1	102	142	9	21	15
	Ahcyl1	64	1017	324	152	190
	C4a	9	120	51	16	33
	Adcyap1r1	9	110	16	40	28
	Tlr3	66	118	28	17	9
	Fcgrt	139	172	54	22	14
	Phyhd1	132	602	105	90	118
	Ckb	357	4334	2061	1070	1179
	Cpne2	14	129	21	37	44
	Tmem100	56	77	13	12	12
	Etv5	183	437	40	131	137
Neurons	*Nefl*	8	29	5	84	294
	Rtn1	39	313	19	782	1126
	Chl1	4	163	14	179	270
	Basp1	535	238	29	1246	1629
	D3Bwg0562	10	115	82	293	435
	Kcnma1	8	62	6	105	158
	Unc13a	14	76	7	174	203
	Gm4392	4	91	11	116	135
	Slc2a3	14	24	4	66	78
	Sez6l	11	34	9	44	110
	Cnrip1	28	89	21	153	267
	Ccnd1	90	9	13	158	129
	Khdrbs3	64	128	30	128	325
	Ctnna2	14	39	93	197	181
	Rab6b	40	93	52	224	253
	Bend6	27	20	12	91	78
	Necap1	49	97	38	150	202
	Rufy3	33	89	168	183	234
	Pgrmc1	73	239	192	319	456
	Ptms	136	206	83	338	430
	Gmfb	76	152	186	294	398
	Myef2	54	121	96	220	248
	Pea15a	111	482	688	842	740
	Gnas	90	223	186	392	419
	Hmgn1	103	196	93	276	321
Microglia	*P2ry12*	4666	25	92	9	4
	Tmem119	2099	4	53	12	6
	Fcrls	965	5	34	13	4
	Olfml3	905	3	18	14	5
	Hexb	8991	103	235	22	27
	Ctss	4101	9	76	15	3
	C1qb	3150	3	62	3	4
	C1qa	2669	5	60	7	3
	Csf1r	2905	4	80	24	7
	P2ry13	1472	2	32	8	7
	Cx3cr1	3836	6	79	21	7
	Gpr34	838	1	16	13	1
	C1qc	4558	8	109	15	8
	Mafb	1382	5	14	18	11
	Tgfbr1	1678	27	75	22	25
	Fcgr1	456	2	14	9	4
	Entpd1	731	21	39	9	4
	Ltc4s	461	4	28	5	3
	Csf3r	294	2	5	12	6
	Il10ra	604	3	15	25	5
	Egr1	1968	163	12	63	58
	Siglech	489	3	17	20	6
	Ccl2	126	1	5	18	6
	Lag3	246	8	11	8	2
	Fos	1806	47	13	39	13

Nature Neuroscience: doi:10.1038/nn.3599

Supplementary Table 2:
Top unique microglial genes and shared genes between microglia, neurons, astrocytes and oligodendrocytes.

Top 40 Microglial unique genes	Microglia/Neuron genes	Microglia/Astrocyte genes	Microglia/Oligodendrocyte genes
P2ry12	*Asph*	*Sall1*	*C1qc*
Tmem119	*Basp1*	*Itgb5*	*C1qb*
Olfml3	*Cd34*	*Cst3*	*C1qa*
P2ry13	*Tanc2*	*Slc1a3*	*Ctss*
Cx3cr1	*Slc7a8*	*Gpr56*	*Timp2*
Gpr34	*Syngr1*	*Mertk*	*Bin1*
Hexb	*Rgmb*	*Cables1*	*Frmd4b*
Rhob	*Npnt*	*Sall3*	*Tmcc3*
Jun	*Mef2a*	*Etv5*	*Chn2*
Rab3il1	*Rtn4rl1*	*Chst7*	*Gab1*
Serpine2	*Mef2c*	*Eya4*	*Spsb1*
Ccl2	*Khdrbs3*	*Arhgap5*	*Slc12a2*
Scoc	*Myo1b*	*Rnf180*	*Scarb2*
Fcrls	*Rtn1*	*Pmp22*	*Pdgfa*
Siglech		*Tmem144*	*Rap1gds1*
Slc2a5		*Npl*	*Pak1*
Lrrc3		*Trim47*	*Epn2*
Plxdc2		*Tlr3*	
Usp2		*Itga6*	
Ctsf		*Abca1*	
Cttnbp2nl		*Tmem100*	
Tgfbr1		*Arhgap12*	
Atp8a2		*Fads1*	
Lgmn		*Spire1*	
Slco2b1		*Tspan7*	
Egr1		*Jam2*	
Mafb		*Lrrc8a*	
Bhlhe41		*Il18*	
Fcgr1a			
Ctsd			
Hpgds			
Hspa1a			
Adamts1			
Lag3			
Csf1r			
F11r			
Golm1			
Nuak1			
Crybb1			
Ltc4s			

Supplementary Table 2. Top unique microglial genes and shared genes between microglia and neurons, astrocytes and oligodendrocytes. The top 40 microglia specific genes are presented. Complete list of 152 microglia enriched genes are shown in Source data – Supplementary Table 2.

Nature Neuroscience: doi:10.1038/nn.3599

Supplementary Table 3:
Top microglia interactions by protein functions

Object Type	Network Object name	Actual	Expected	Ratio	p-value
Transcription factors	PU.1	46	15.36	2.994	3.67E-11
	GCR-alpha	69	30.73	2.245	2.00E-10
	GATA-1	61	26.61	2.292	1.18E-09
	SP1	127	76.84	1.653	2.10E-09
	ETS2	28	7.537	3.715	2.88E-09
	HIF1A	47	19.03	2.469	1.19E-08
	CREB1	69	34.24	2.015	1.77E-08
	RelA (p65 NF-kB subunit)	59	27.55	2.141	2.70E-08
	NF-kB1 (p50)	35	12.35	2.835	3.54E-08
	MafB	15	2.572	5.832	4.33E-08
	C/EBPbeta	56	26.14	2.142	6.27E-08
	ETS1	48	20.89	2.298	7.57E-08
	SP3	35	12.79	2.736	8.49E-08
	c-Jun	54	25.38	2.127	1.38E-07
	BATF	11	1.454	7.567	1.88E-07
	STAT1	37	15.72	2.353	1.46E-06
	C/EBPalpha	44	20.84	2.111	2.64E-06
	p63	35	14.83	2.36	2.65E-06
	Elk-3	7	0.6486	10.79	2.73E-06
	PEA3	26	9.348	2.781	2.99E-06
Ligands	CCL8	7	0.5591	12.52	9.07E-07
	APOA1	11	2.55	4.314	5.05E-05
	TGF-beta 3	6	0.7157	8.384	6.70E-05
	Endostatin	7	1.096	6.388	1.02E-04
	TGF-beta 1	12	3.377	3.553	1.54E-04
	Cyr61	8	1.7	4.707	2.94E-04
	VIP	5	0.6486	7.709	4.17E-04
	LAMA2	3	0.1789	16.77	5.72E-04
	LIF	5	0.6933	7.212	5.75E-04
	SDF-1	7	1.543	4.536	8.73E-04
	CCL2	8	2.035	3.931	9.89E-04
	Galanin	4	0.4697	8.517	1.09E-03
	MIP-1-beta	5	0.8499	5.883	1.50E-03
	LAMC3	4	0.5144	7.776	1.56E-03
	LL37	5	0.9169	5.453	2.11E-03
	CCL13	5	0.9169	5.453	2.11E-03
	APOE	9	2.84	3.169	2.24E-03
	Fibrillin 1	7	1.879	3.726	2.75E-03
	FasL(TNFSF6)	9	2.93	3.072	2.77E-03
	IP10	6	1.431	4.192	3.04E-03
Receptors	Agtr1b	5	0.3131	15.97	9.28E-06
	Tissue factor	8	1.141	7.014	1.61E-05
	AGTR1	10	1.923	5.199	2.20E-05
	ITGB4	9	1.566	5.749	2.51E-05
	CXCR6	3	0.08946	33.54	4.37E-05
	CD9	10	2.192	4.563	6.87E-05
	BAMBI	5	0.492	10.16	1.05E-04
	TREM1	4	0.2907	13.76	1.50E-04
	CCR4	4	0.2907	13.76	1.50E-04
	ITGB1	16	5.613	2.85	1.81E-04
	Neuropilin-2	6	0.8946	6.707	2.44E-04
	VEGFR-2	12	3.578	3.354	2.64E-04
	EGFR	28	13.75	2.036	3.28E-04
	LDLR	7	1.364	5.131	4.11E-04
	ITGB8	4	0.3802	10.52	4.66E-04
	Endoglin	6	1.029	5.832	5.32E-04
	A2M receptor	13	4.428	2.936	5.40E-04
	PTPRO	6	1.051	5.708	5.98E-04
	Plexin B1	5	0.738	6.775	7.75E-04
	TGF-beta receptor type III (betaglycan)	7	1.521	4.603	8.00E-04
Enzymes	p300	40	21	1.905	7.76E-05
	JMJD3	14	4.182	3.348	8.49E-05
	MTCBP-1	3	0.1342	22.36	2.11E-04
	GCL cat	7	1.23	5.691	2.15E-04
	AOX1	5	0.5815	8.599	2.44E-04
	PLC-gamma 2	9	2.102	4.281	2.56E-04
	AK1BA	4	0.3355	11.92	2.77E-04
	GGT1	5	0.6038	8.28	2.94E-04
	FTase-alpha	5	0.6262	7.985	3.52E-04
	GNT-V	6	0.984	6.097	4.16E-04
	HPGD	4	0.4026	9.936	5.89E-04
	PLD2	7	1.476	4.742	6.67E-04
	PSAT	4	0.4249	9.413	7.33E-04
	NRHQR2	4	0.4249	9.413	7.33E-04
	TPST1	3	0.2013	14.9	8.44E-04
	TGM2	12	4.137	2.9	9.71E-04
	GAD1	5	0.8051	6.21	1.17E-03
	MAG1	3	0.2236	13.41	1.19E-03
	DPYD	4	0.492	8.13	1.31E-03
	SYVN1	11	3.713	2.963	1.31E-03
Kinases	p90RSK1	9	1.655	5.438	3.95E-05
	TSSK1	3	0.08946	33.54	4.37E-05
	JAK1	12	3.064	3.917	6.05E-05
	c-Src	29	13.49	2.15	1.02E-04
	FAK1	16	5.725	2.795	2.26E-04
	p38alpha (MAPK14)	17	6.396	2.658	2.63E-04
	VEGFR-2	12	3.578	3.354	2.64E-04
	EGFR	28	13.75	2.036	3.28E-04
	DYRK1a	9	2.281	3.945	4.72E-04
	p90RSK3(RPS6KA2)	5	0.738	6.775	7.75E-04
	TGF-beta receptor type III (betaglycan)	7	1.521	4.603	8.00E-04
	BMP receptor 2	8	2.013	3.975	9.20E-04
	Csk	12	4.249	2.824	1.22E-03
	PI3K cat class IA (p110-alpha)	8	2.214	3.613	1.71E-03
	TGF-beta receptor type II	10	3.355	2.981	2.06E-03
	KCRS	3	0.2684	11.18	2.10E-03
	MSK1	5	0.9393	5.323	2.36E-03
	ErbB2	11	4.048	2.717	2.60E-03

Nature Neuroscience: doi:10.1038/nn.3599

Supplementary Table 4:
Top microglial upstream regulators based on genearray profile identified by IPA™

Upstream Regulator	Molecule Type	Predicted Activation State	Activation z-score	p-value of overlap
SMAD3	TR	Activated	3.569	6.74E-09
Ap1	complex	Activated	3.249	2.13E-07
SP1	TR	Activated	3.532	3.56E-07
EGR1	TR	Activated	2.479	4.06E-07
AR	ligand-dependent nuclear receptor	Activated	2.513	5.70E-06
ELK1	TR	Activated	2.357	6.50E-06
JUN	TR	Activated	2.39	9.42E-06
NFkB (complex)	complex	Activated	4.64	1.32E-05
EGR2	TR	Activated	2.94	1.76E-05
NFYA	TR	Activated	2.121	2.49E-05
NFKBIA	TR	Activated	2.824	2.63E-05
STAT4	TR	Activated	3.841	3.99E-05
NFATC2	TR	Activated	2.155	4.56E-05
MITF	TR	Activated	2.447	6.82E-05
ETS1	TR	Activated	2.918	8.05E-05
ARNT2	TR	Activated	3.742	1.05E-04
STAT3	TR	Activated	3.52	1.13E-04
RELA	TR	Activated	2.911	1.20E-04
SIM1	TR	Activated	3.742	1.42E-04
HIF1A	TR	Activated	2.389	1.61E-04
NFKB1	TR	Activated	2.615	1.65E-04
CEBPB	TR	Activated	2.315	2.18E-04
SMAD7	TR	Inhibited	-2.739	8.92E-07
KLF2	TR	Inhibited	-2.002	3.87E-06
IKZF1	TR	Inhibited	-3.162	6.22E-05
CBFB	TR	Inhibited	-2.121	1.00E-04
DACH1	TR	Inhibited	-2.2	1.16E-04
miR-29b-3p	mature microRNA	Inhibited	-2.183	8.12E-03
HOXA10	TR	Inhibited	-2.333	1.32E-02
miR-155-5p	mature microRNA	Inhibited	-2.789	1.33E-02
miR-16-5p	mature microRNA	Inhibited	-2.921	1.42E-02
miR-1	mature microRNA	Inhibited	-2.97	2.31E-02
MYC	TR	Inhibited	-2.28	2.76E-02
GFI1	TR	Inhibited	-2.236	3.22E-02

* TR, transcription regulator

Nature Neuroscience: doi:10.1038/nn.3599